

Theoretical Aspects of Differential Reflectance and Electreflectance Spectroscopy in the UV–Vis Region As Applied to the Study of Molecular Layers Adsorbed on Metal Surfaces

Sunghyun Kim,[†] Zhenghao Wang,[‡] and Daniel A. Scherson^{*‡}

Department of Chemistry, Konkuk University, Seoul 143-701, Korea, and Department of Chemistry, Case Western Reserve University, Cleveland, Ohio 44106

Received: August 30, 1996; In Final Form: February 1, 1997[®]

Differential reflectance UV–vis spectra ($\Delta R/R$ vs wavelength, λ) of molecular layers adsorbed on various metal surfaces have been simulated using Fresnel equations for a stratified three-phase model for the interface, assuming each constituent retains its bulk optical properties after the interface is formed, i.e. *total neglect of adsorbate–substrate interactions*. Results obtained for ultrathin films (1 nm) of squarylium, *meso*-tetrakis-(phenylporphyrin), and metal-free phthalocyanine in contact with Au, Pt, and the basal plane of highly oriented pyrolytic graphite have shown that the shape of $\Delta R/R$ vs λ for p-polarized light depends quite markedly on the angle of incidence and the optical constants of the substrate. At normal incidence, the reflectance spectra displayed peaks similar to those observed in the conventional absorption spectra of the materials. As the angle was increased, however, the position of these features not only shifted, but, in certain cases, new bands emerged, which could not be readily ascribed to the overlayer. This indicates that *under non-normal incidence conditions, no conclusions regarding the physical state of adsorbed monolayers on metal substrates can be drawn on the basis of a cursory examination of $\Delta R/R$ vs λ curves in this spectral region*. These purely optical effects may also account for features observed in the electreflectance spectra of monolayers irreversibly adsorbed on electrode surfaces, in which case the reflectivity of the substrate is modified by its state of charge.

I. Introduction

The reflectivity of metals in the UV–vis spectral region can be influenced significantly by their surface microtopography and state of charge, as well as by the adsorption of species on the surface.¹ Advantage has been taken of this effect to examine various phenomena at electrode/electrolyte interfaces, including the dynamics of surface reconstruction,² electronic transitions involving surface states,³ oxide formation on noble metal surfaces,⁴ and ionic,⁵ atomic,⁶ and molecular adsorption.^{7,8} For many adsorbates, even at submonolayer coverages, the normalized reflectivity, defined as $\Delta R/R = (R_{\text{ads}} - R)/R$, where R_{ads} and R are the intensities of the reflected light from the surface in the presence and in the absence of the adsorbate, respectively, can reach values on the order of 1%, which are well within the sensitivity range of simple optical instrumentation. Not surprisingly, UV–vis reflectance spectroscopy has gained considerable popularity in the electrochemical area, as evidenced by the growing number of papers published in the literature.⁹

Of special interest is to extract from the reflectance (or electreflectance) data information regarding the mode of adsorption of species to electrode surfaces and the effects of the applied field on the electronic and structural characteristics of the adsorbate. Considerable care must be exercised in the interpretation of the results of such measurements since the *normalized reflectivity spectra of the metal/adsorbate/electrolyte interface may not resemble the transmission spectra of the adsorbed layer even in the absence of any chemical interactions*. In other words, the interface cannot be regarded as an absorber (adsorbate phase) placed in front of a simple mirror (underlying substrate), so that the spectrum of the adsorbate can be obtained by simply subtracting the reflected signal observed in the

presence of the overlayer from that obtained for the bare substrate under otherwise identical experimental conditions. This conclusion may be derived from the analysis of the optical response of a stratified three-phase media based on classical electromagnetic theory, which predicts that $\Delta R/R$ is a complex function of the angle of incidence and the optical properties of the adsorbed phase, the metal, and the electrolyte.

This work examines modifications in the optical response of carefully selected adsorbate/substrate interfacial systems as a function of the angle of incidence, to illustrate the marked differences that exist between the conventional transmission spectrum of the adsorbate and the reflection spectrum of the interface *under conditions in which adsorbate–substrate interactions are fully neglected*. Simple examples of this phenomenon have been given by Kotz and Kolb^{1b} and much earlier by McIntyre.^{1a} Also included in this study are the effects associated with adsorbates and substrates that display anisotropic optical constants.

On the basis of the results of these classical optics simulations, it may be ascertained that *no conclusions can be made regarding the state of the adsorbate on the surface of a moderate to good electronic conductor in the UV–visible range by a cursory comparison of the reflection–absorption spectrum with that observed for the adsorbate in a conventional transmission-type experiment*.

These effects also introduce complications in the analysis of electreflectance data of adsorbed monolayers, as evidenced by optical simulations involving a primitive model for charged interfaces that incorporates, albeit in a simple fashion, some of the essential features of this phenomenon.

II. Three-Phase Optical Model of Electrode/Adsorbate/Electrolyte Interfaces

From a strictly optical viewpoint, the metal/adsorbate/electrolyte system can be regarded as a stratified media

[†] Konkuk University.

[‡] Case Western Reserve University.

[®] Abstract published in *Advance ACS Abstracts*, March 15, 1997.

consisting of three homogeneous (*vide infra*) phases separated by sharp, flat, and parallel boundaries: the electrolyte, the electrode, and a third phase interposed between these two phases representing the adsorbate. The magnitudes of the electric field vectors of the incident, transmitted, and reflected plane waves at any point within multilayered structures of such type, involving materials with arbitrary anisotropic properties, can be determined from Yeh's 4×4 matrix algebra.¹⁰

The dimensions of atoms and molecules, however, are about 3 orders of magnitude smaller than the wavelength of light in the UV–vis spectral region. Under such conditions it becomes possible to linearize Fresnel equations for a three-phase stratified system, yielding, as shown originally by Aspnes and McIntyre,¹¹ a much simpler set of equations that describe with high accuracy the optical response of the interface. For systems involving isotropic media, the normalized reflectivities for s-, and p-polarizations may be shown to be given by

$$(\Delta R/R)_s = (8\pi d n_1 \cos \phi_1 / \lambda) \operatorname{Im}\{[(\hat{\epsilon}_2 - \hat{\epsilon}_3)/(\hat{\epsilon}_1 - \hat{\epsilon}_3)]\} \quad (1)$$

$$(\Delta R/R)_p = (8\pi d n_1 \cos \phi_1 / \lambda) \operatorname{Im}\{[(\hat{\epsilon}_2 - \hat{\epsilon}_3)/(\hat{\epsilon}_1 - \hat{\epsilon}_3)]\} W \quad (2)$$

where

$$W = \frac{1 - [(\hat{\epsilon}_1)/(\hat{\epsilon}_2 \hat{\epsilon}_3)][\hat{\epsilon}_2 + \hat{\epsilon}_3] \sin^2 \phi_1}{1 - (1/\hat{\epsilon}_3)[\hat{\epsilon}_1 + \hat{\epsilon}_3] \sin^2 \phi_1} \quad (3)$$

and d is the thickness of the adlayer; ϕ_1 , the angle of incidence; λ , the wavelength of the incident light; $\hat{\epsilon}_i$, the complex, wavelength dependent dielectric constant of phase i ; and Im , the imaginary part of the complex number. This simpler linearized approach will be used in the following sections to examine the optical response of a variety of model interfaces.

III. $\Delta R/R$ vs λ Simulations of Selected Metal/Adsorbate/Electrolyte Systems

The model systems chosen for this study involve substrates and adsorbates for which the optical constants have been determined with high accuracy; specifically, highly ordered pyrolytic graphite (HOPG),^{12a} Au,¹³ and Pt¹³ as the substrates and squarylium (SQ),¹⁴ *meso*-tetrakis(phenyl) porphyrin (TPP),¹⁵ and (metal-free) phthalocyanine (Pc)¹⁵ as the adsorbates. This section explores the effects of the incidence angle, ϕ_1 , and the optical properties of the adsorbate and the substrate, either isotropic or uniaxial, on the normalized UV–visible reflectance spectra ($\Delta R/R$ vs λ).

It will be assumed in what follows that the electrolyte is isotropic and nonabsorbing ($k = 0$) with energy independent optical constants. All simulations were performed with p-polarized light only.

a. Effect of Film Anisotropy. Squarylium (SQ) is one of the few molecular species for which both anisotropic (ani) and *effective* isotropic (iso) optical constants have been reported in the literature¹⁴ (see panels A and B in Figure 1, respectively); hence, it may be regarded as a model adsorbate to explore the effect of film anisotropy on the optical behavior of the interface. Certain aspects of this phenomenon have been studied, from a more general perspective, by Dignam et al.,¹⁶ who first noted that the use of *effective* isotropic optical constants to represent a uniaxial molecular layer with its c -axis normal to the substrate can lead to significant errors in $\Delta R/R$.

The optical simulations involved HOPG as a substrate, a well-characterized, uniaxial, layered material that exhibits unique optical (see panel C, Figure 1),^{12a} electronic,^{12b} and electrochemical^{12c} properties, with its basal plane (bp) oriented parallel

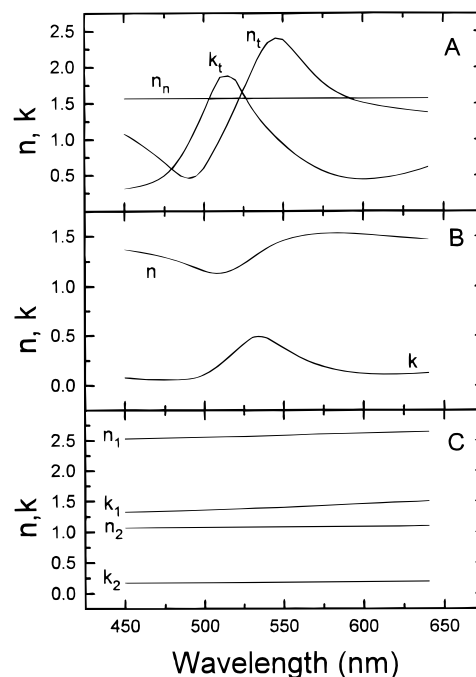


Figure 1. Anisotropic (panel A) and *effective* isotropic (panel B) optical constants for squarylium (SQ) (adapted from ref 14). Panel C shows the anisotropic optical constants of HOPG (adapted from ref 12a).

to the interface. Within the linear approximation, the expressions for $(\Delta R/R)_p$ and $(\Delta R/R)_s$ for an anisotropic film in contact with an anisotropic substrate are given by

$$(\Delta R/R)_s = (8\pi d n_1 \cos \phi_1 / \lambda) \operatorname{Im}\{[(\hat{\epsilon}_{2t} - \hat{\epsilon}_{3t})/(\hat{\epsilon}_1 - \hat{\epsilon}_{3t})]\} \quad (4)$$

$$(\Delta R/R)_p = (8\pi d n_1 \cos \phi_1 / \lambda) \operatorname{Im}\{[(\hat{\epsilon}_{2t} - \hat{\epsilon}_{3t})/(\hat{\epsilon}_1 - \hat{\epsilon}_{3t})]\} W \quad (5)$$

where

$$W = \frac{1 - [(\hat{\epsilon}_1)/(\hat{\epsilon}_{2t} - \hat{\epsilon}_{3t})][(\hat{\epsilon}_{2t}/\hat{\epsilon}_{3n}) - (\hat{\epsilon}_{3t}/\hat{\epsilon}_{2n})] \sin^2 \phi_1}{1 - [(\hat{\epsilon}_1^2 - \hat{\epsilon}_{3t}\hat{\epsilon}_{3n})/(\hat{\epsilon}_{3n}(\hat{\epsilon}_1 - \hat{\epsilon}_{3t}))] \sin^2 \phi_1} \quad (6)$$

and the subscripts t and n indicate values of $\hat{\epsilon}_i$ parallel and normal to the graphite planes, respectively.

Plots of $(\Delta R/R)_p$ vs λ for HOPG(bp)/SQ(ani, $d=1$ nm)/water and HOPG(bp)/SQ(iso, $d=1$ nm)/water in the range 450–640 nm, for various values of ϕ_1 , are shown in panels A and B of Figure 2. Careful inspection of these curves reveals a number of interesting facts:

(i) Pronounced changes in the shape of the $\Delta R/R$ vs λ are observed as ϕ_1 is varied over the range $0 < \phi_1 < 70^\circ$, regardless of the specific model used to represent the optical constants of the adsorbate.

(ii) No direct correspondence can be discerned between the k vs λ (see panel B, Figure 2) and $(\Delta R/R)_p$ vs λ spectra of the HOPG(bp)/SQ(iso, $d=1$ nm) water system for $\phi_1 > 0$. For $\phi_1 = 0$, however, $(\Delta R/R)_p$ vs λ does indeed resemble the absorption spectra of SQ(iso).

(iii) Clear differences are found between $(\Delta R/R)_p$ vs λ as a function of ϕ_1 between HOPG(bp)/SQ(ani, $d=1$ nm)/water and HOPG(bp)/SQ(iso, $d=1$ nm)/water, as illustrated more clearly by the three-dimensional plots in panels A and B of Figure 3, respectively.

b. Effect of Substrate Reflectivity on $\Delta R/R$. The reflectivity of gold in the wavelength region above 550 nm is very high, dropping by about 70% at higher energies (see Figure 4

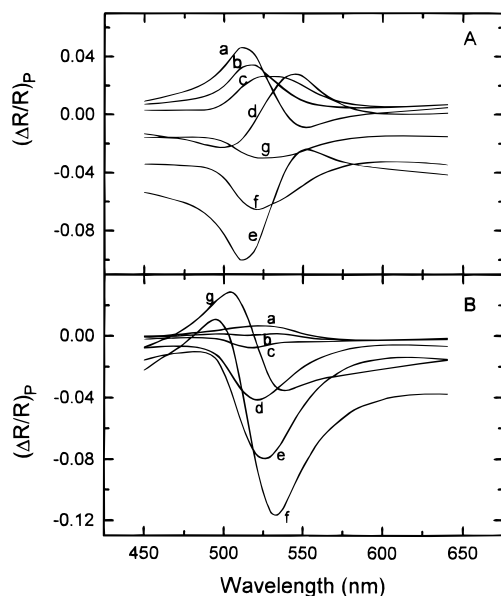


Figure 2. Plots of $(\Delta R/R)_p$ vs λ for HOPG(bp)/SQ(ani, $d=1$ nm)/water (panel A: curve a, $\phi_1 = 0^\circ$; b, 40° ; c, 50° ; d, 60° ; e, 70° ; f, 80° ; g, 85°) and HOPG(bp)/SQ(iso, $d=1$ nm)/water (panel B: curve a, $\phi_1 = 0^\circ$; b, 20° ; c, 30° ; d, 50° ; e, 60° ; f, 70° ; g, 80°) for various values of ϕ_1 .

for $\phi_1 = 60^\circ$). This property provides ideal conditions for examining the effects of the substrate reflectivity on the optical behavior of the interface. Two different materials in the form of films 1 nm thick were selected for these simulations:

- (i) metal-free phthalocyanine (Pc), a compound that exhibits an intense band centered at 680 nm, i.e. within the energy range in which Au is a good reflector (see panel A, Figure 5), and
- (ii) *meso*-tetrakis(phenylporphyrin) (TPP), a material that displays a strong absorption band centered at 420 nm (see panel A, Figure 6), a region in which Au shows much lower reflectivity.

In analogy with the results obtained for SQ(iso) on HOPG(bp), only at ϕ_1 ca. 0, $(\Delta R/R)_p$ vs λ for the Au/Pc(1 nm)/water interface displayed transmission-like Pc characteristics, whereas strong spectral distortions were observed at higher angles of incidence (see panel B, Figure 5).

A much more complex behavior was found for Au/TPP(1 nm)/water, given in panel B, Figure 6. Specifically, the feature centered at ca. 420 nm, the prominent peak in the absorption spectrum of this material, was found to change sign as ϕ_1 was varied. More surprising, however, was the emergence of a second peak at about 400 nm, an energy range in which the conventional absorption spectrum of TPP displays no special features.

A very complicated angle dependence was also observed for the reflectance spectra of both TPP and Pc upon changing the substrate from Au to Pt and HOPG(bp), two electrode materials for which the optical constants do not vary rapidly as a function of energy over a large spectral region. A comparison of $(\Delta R/R)_p$ vs λ for Au/TPP(1 nm)/water with the Pt/TPP(1 nm)/water and HOPG(bp)/TPP(1 nm)/water systems for $\phi_1 = 0^\circ$ (thin line) and 60° (thick line) is given in panels A–C of Figure 7, respectively.

IV. Electrorreflectance Effects

As was mentioned in the Introduction, the reflectivity of metals in the UV–vis spectral region can be significantly affected by their state of charge. This phenomenon, known as *intrinsic electrorreflectance* (see below), has been studied in

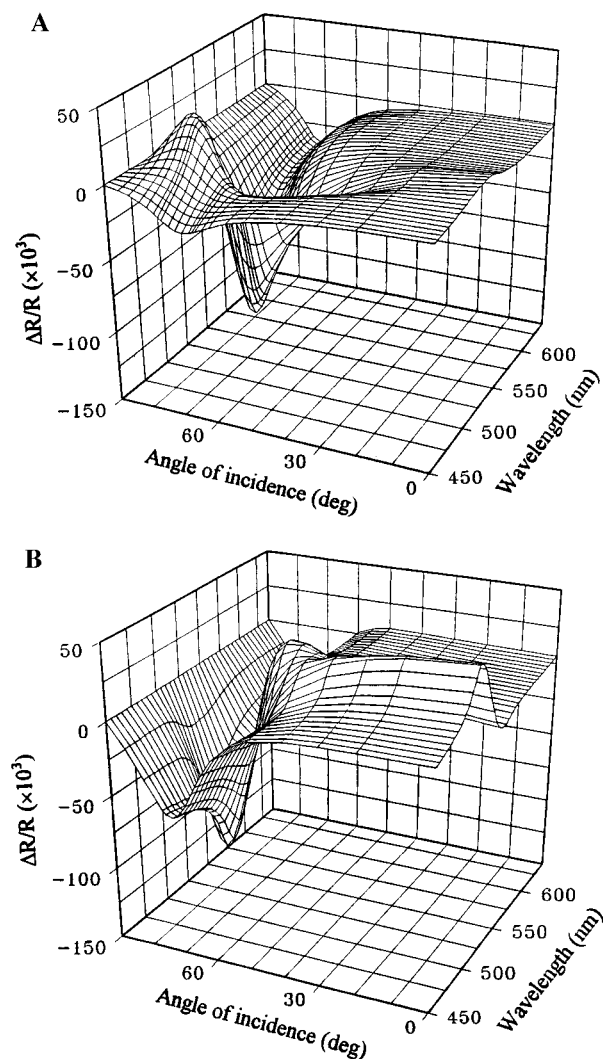


Figure 3. Three-dimensional plots of $(\Delta R/R)_p$ as a function of wavelength and angle of incidence (ϕ_1) for HOPG(bp)/SQ(iso, $d=1$ nm)/water (panel A) and HOPG(bp)/SQ(ani, $d=1$ nm)/water (panel B) based on the data shown in Figure 2.

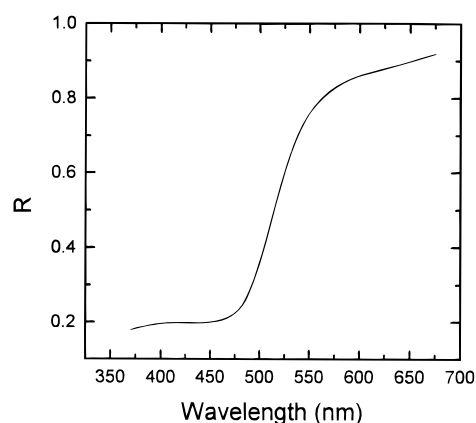


Figure 4. Reflectivity of gold in air as a function of wavelength for $\phi_1 = 60^\circ$.

detail for a number of metals, particularly Au in aqueous electrolytes.¹ Modifications in the interfacial reflectivity have also been observed in the case of molecular layers irreversibly adsorbed on metal electrode surfaces upon changing the applied potential.^{7,8} Much of the work in this specific area has focused on redox active molecular layers, for which the reflectivity of the interface is markedly altered as the material changes oxidation state.⁷ However, more subtle effects have been found

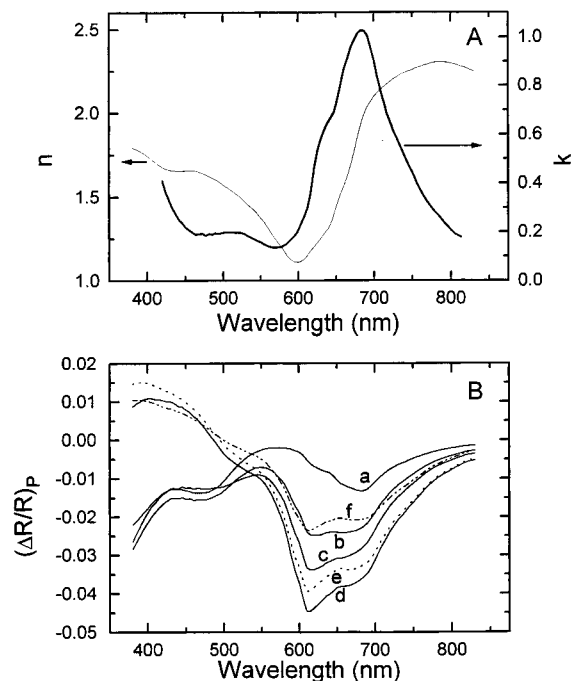


Figure 5. (A) Optical constants (n , k) of PC as a function of wavelength (adapted from ref 15). (B) Plots of $(\Delta R/R)_p$ vs λ for the Au/PC(1 nm)/water system for various values of ϕ_1 . Curve a, $\phi_1 = 0^\circ$; b, 40° ; c, 50° ; d, 60° ; e, 76° ; f, 83° .

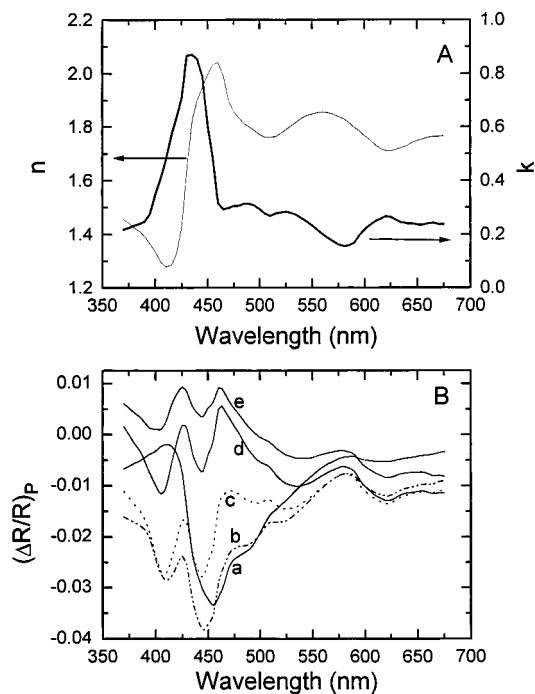


Figure 6. (A) Optical constants (n , k) of TPP as a function of wavelength (adapted from ref 15). (B) Plots of $(\Delta R/R)_p$ vs λ for the Au/TPP(1 nm)/water system for various values of ϕ_1 . Curve a, $\phi_1 = 0^\circ$; b, 30° ; c, 60° ; d, 70° ; e, 80° .

for such interfacial systems at potentials at which the layers display no redox activity, and for non-redox active films over a wide voltage range.⁸ This phenomenon has been explained in terms of interactions between the electric field at the interface and the film, which can change the electronic properties of the molecular species, as well as the angle(s) the dipole moment(s) makes with respect to the surface normal (geometric reorientation), known generically as electrochromism.¹⁷

Since changes in the state of charge of the substrate may be expected to modify its optical properties, it is of interest to

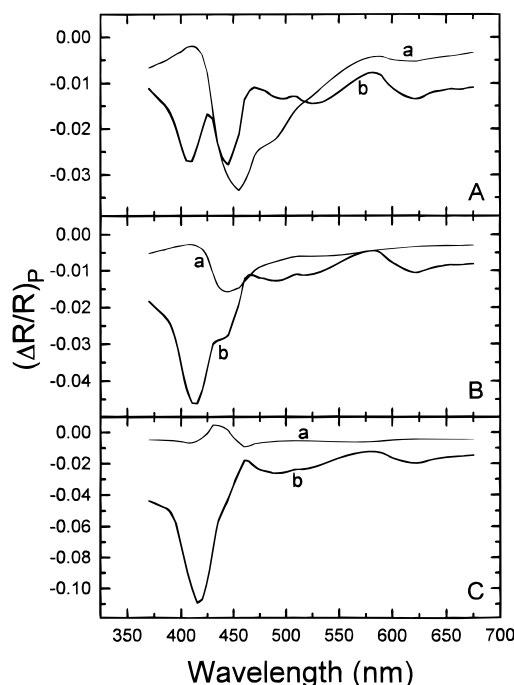


Figure 7. Comparison of $(\Delta R/R)_p$ vs λ curves for Au/TPP(1 nm)/water (panel A), Pt/TPP(1 nm)/water (panel B), and HOPG(bp)/TPP(1 nm)/water (panel C) systems for $\phi_1 = 0^\circ$ (thin line, a) and 60° (thick line, b).

explore whether the electroreflectance data for some of the substrate/adsorbate/electrolyte systems reported to date can be qualitatively accounted for by purely optical rather than electrochromic effects.

The primitive model to be described in the following section represents a first attempt at assessing possible contributions of the intrinsic electroreflectance effect to the observed electroreflectance spectra of adsorbed layers on gold electrode surfaces in aqueous electrolytes.

(a) Primitive Electroreflectance Model for Metal/Adsorbate/Electrolyte Interfaces. The starting point of this analysis considers a system that consists of four noninteracting phases: a metal substrate with dielectric function $\hat{\epsilon}_4$, two adsorbate films with dielectric functions $\hat{\epsilon}_3$ and $\hat{\epsilon}_2$ and thickness d_3 and d_2 , respectively, and a nonabsorbing (purely real $\hat{\epsilon}_1 = n_1^2$) electrolyte, arranged in that order. Takamura et al.¹⁸ have shown that, provided d_2 and d_3 are much smaller than the wavelength of light λ , the change in reflectivity of the substrate/electrolyte two-phase system, i.e. 4, 1, induced by the presence of the two films, 2 and 3, is given by

$$(\Delta R/R_0)_s = (8\pi d_2 n_1 \cos \phi_1 / \lambda) \operatorname{Im}\{[(\hat{\epsilon}_2 - \hat{\epsilon}_4)/(n_1^2 - \hat{\epsilon}_4)]\} + (8\pi d_3 n_1 \cos \phi_1 / \lambda) \operatorname{Im}\{[(\hat{\epsilon}_3 - \hat{\epsilon}_4)/(n_1^2 - \hat{\epsilon}_4)]\} \quad (7)$$

$$(\Delta R/R_0)_p = (8\pi d_2 n_1 \cos \phi_1 / \lambda) \operatorname{Im}\{[(\hat{\epsilon}_2 - \hat{\epsilon}_3)/(n_1^2 - \hat{\epsilon}_3)]\} W_2 + (8\pi d_3 n_1 \cos \phi_1 / \lambda) \operatorname{Im}\{[(\hat{\epsilon}_3 - \hat{\epsilon}_4)/(n_1^2 - \hat{\epsilon}_4)]\} W_3 \quad (8)$$

where

$$W_2 = \frac{1 - [n_1^2 / (\hat{\epsilon}_2 \hat{\epsilon}_4)] [\hat{\epsilon}_2 + \hat{\epsilon}_4] \sin^2 \phi_1}{1 - (1/\hat{\epsilon}_4) [n_1^2 + \hat{\epsilon}_4] \sin^2 \phi_1} \quad (9)$$

$$W_3 = \frac{1 - [n_1^2 / (\hat{\epsilon}_3 \hat{\epsilon}_4)] [\hat{\epsilon}_3 + \hat{\epsilon}_4] \sin^2 \phi_1}{1 - (1/\hat{\epsilon}_4) [n_1^2 + \hat{\epsilon}_4] \sin^2 \phi_1} \quad (10)$$

and R_0 is the reflectivity of the substrate/electrolyte, 4|1, two-phase interface.

According to these equations, the overall change in reflectivity may be regarded as arising from additive contributions due to two three-phase systems, i.e. 4|2|1 and 4|3|1 (see eqs 1–3) and, therefore, independent of whether 2 or 3 is immediately adjacent to the substrate. The validity of the linear approximation for a four-phase system was verified by comparing the results of Au/TPP(1 nm)/PC(1 nm)/water with those obtained using the rigorous four-phase expression,¹⁰ yielding excellent agreement (within 5%).

It will be further assumed that phase 3 represents the transition region between the metal substrate and the electrolyte, as prescribed by the intrinsic electroreflectance model of McIntyre and Aspnes.¹ According to their analysis, the expression for the normalized reflectivity change for s-light due to a change in the applied potential, in the absence of an adsorbate layer, may be shown to be given by

$$(\Delta R/R_0)_s = (8\pi d_3 n_1 / \lambda) \cos \phi_1 \operatorname{Im}\{[(\hat{\epsilon}_3 - \hat{\epsilon}_4)/(n_1^2 - \hat{\epsilon}_4)]\} = (8\pi d_3 n_1 / \lambda) \cos \phi_1 \operatorname{Im}\{\langle \Delta \hat{\epsilon} \rangle / (n_1^2 - \hat{\epsilon}_4)\} \quad (11)$$

where

$$\langle \Delta \hat{\epsilon} \rangle = (\hat{\epsilon}_f - 1)(\Delta N / d_3 N) \quad (12)$$

The term $\hat{\epsilon}_f$ in eqs 11 and 12 represents the dielectric function of the free electrons in the metal, ΔN is the excess electrons due to a change in potential with respect to the pzc, i.e. $\Delta N = N(E) - N$, where $E = E' - E(\text{pzc})$, N is the free-electron concentration of the bare uncharged metal, and E' is the actual potential applied to the electrode. On the basis of this formalism, for $E = E_{\text{pzc}}$, $\Delta N = 0$, and the change in reflectivity of the interface $(\Delta R/R_0)$ in eqs 7 and 8 above reduces to that in eqs 1–3 for the stratified layered system 4|2|1 for s-light.

Consider an experiment aimed at measuring the change in the optical response of an uncharged substrate/adsorbate/electrolyte (4|2|1) system induced by applying a potential E . A quantity amenable to experimental determination is the normalized change in reflectivity, i.e.

$$(\Delta R/R)_E = \{R(E) - R(E_{\text{pzc}})\} / R(E_{\text{pzc}}) \quad (13)$$

where $R(E)$ is the reflectivity at any arbitrary potential E . Further insight into this expression can be obtained by dividing each term on the right-hand side of eq 7 by R_0 , as defined above, to yield

$$(\Delta R/R)_{s,E} = \{R(E)/R_0 - R(E_{\text{pzc}})/R_0\} / [R(E_{\text{pzc}})/R_0] \quad (14)$$

In general

$$(\Delta R/R_0) = \{R(E) - R_0\} / R_0 = R(E)/R_0 - 1 \quad (15)$$

or

$$R(E)/R_0 = (\Delta R/R_0) + 1 \quad (16)$$

Hence, from eq 7 or 8 and eqs 11 and 12

$$[R(E)/R_0] = (8\pi d_2 n_1 / \lambda) \cos \phi_1 \operatorname{Im}\{[(\hat{\epsilon}_2 - \hat{\epsilon}_4)/(n_1^2 - \hat{\epsilon}_4)]\} + (8\pi n_1 / \lambda)(\Delta N / N) \cos \phi_1 \operatorname{Im}\{(\hat{\epsilon}_f - 1)/(n_1^2 - \hat{\epsilon}_4)\} + 1 \quad (17)$$

and at $E = E_{\text{pzc}}$

$$[R(E_{\text{pzc}})/R_0] = (8\pi d_2 n_1 / \lambda) \cos \phi_1 \operatorname{Im}\{[(\hat{\epsilon}_2 - \hat{\epsilon}_4)/(n_1^2 - \hat{\epsilon}_4)]\} + 1 = (\Delta R/R)_{2,s} + 1 \quad (18)$$

and therefore

$$[(\Delta R/R)]_{s,E} = (8\pi n_1 / \lambda) \cos \phi_1 \operatorname{Im}\{(\hat{\epsilon}_f - 1)(\Delta N / N)/(n_1^2 - \hat{\epsilon}_4)\} / \{(\Delta R/R)_{2,s} + 1\} \quad (19)$$

where $(\Delta R/R)_{2,s}$ is the normalized reflectivity change of the 4|1 two-phase system due to the presence of the adsorbate layer, 2, at the pzc. Furthermore, since $\{(\Delta R/R)_{2,s} \ll 1, (\Delta R/R)_{s,E}$ can be approximated by

$$(\Delta R/R)_{s,E} = (8\pi n_1 / \lambda) \cos \phi_1 \operatorname{Im}\{(\hat{\epsilon}_f - 1)(\Delta N / N)/(n_1^2 - \hat{\epsilon}_4)\} \times \{1 - (\Delta R/R)_{2,s}\} \quad (20)$$

It is evident from this equation that in the absence of the film (layer 2) $(\Delta R/R)_{s,E}$ reduces, as expected, to the expression for the intrinsic ER effect as defined above.

If the interfacial capacity of the metal does not show a very strong dependence on the applied potential, as is the case with polycrystalline gold, this primitive model would predict that the magnitude of $\Delta R/R$, at a fixed wavelength, will be

- (i) independent of the bias potential,
- (ii) directly proportional to ΔN and, hence, to the modulation amplitude, and
- (iii) larger for p-light compared to s-light.

All these predictions are borne out by experiments reported by Lezna et al.⁸ for methylene blue (MB) adsorbed on sulfur-modified gold electrodes in aqueous electrolytes in a potential range in which MB does not undergo changes in oxidation state. Unfortunately, a complete set of optical constants does not seem to be available for this specific compound, making it very difficult to simulate $(\Delta R/R)_{E,s}$ vs λ curves and compare them with experimental data. Nevertheless, some insight into the magnitude and shape of such curves can be obtained using a layer of nonmetalated phthalocyanine (PC), a compound that displays a rather prominent peak in the red end of the spectrum (600–800 nm), i.e. in about the same region as MB (540–770 nm), interposed between gold and water.

Panel A of Figure 8 shows an intrinsic electroreflectance (ER) curve based on the model of McIntyre and Aspnes for $\Delta Q_m = +30 \mu\text{C}/\text{cm}^2$ in the region 500–830 nm at $\phi_1 = 45^\circ$, i.e. the first term in eq 20 (see light line), based on accepted values for ω_p , τ , and N for this metal. Also shown in this figure is a plot of $1 + (\Delta R/R)_{2,s}$ vs λ (see thick line), i.e. the second term in eq 20, where $(\Delta R/R)_{2,s}$ is the normalized reflectivity of the Au-(pzc)/PC(1.5 nm)/water at the same angle of incidence (see thick line).

The corresponding ER curves for the Au(+30 $\mu\text{C}/\text{cm}^2$)/PC-(d_{PC})/water system for $d_{\text{PC}} = 30$ and 45 nm are shown in panel B in the same figure, which includes the *intrinsic* ER curve from panel A, for comparison. As indicated, the ER curves show clear features attributed to the presence of PC on Au. It must be stressed that the magnitude and shapes of these curves are smaller than those expected experimentally. Such discrepancy is due in part to the fact that the McIntyre–Aspnes model predicts values for the intrinsic electroreflectance effect about an order of magnitude smaller than those found experimentally in the lower energy range.¹ Also to be noted is the fact that the normalized reflectivity at $\phi_1 = 45^\circ$ for systems involving

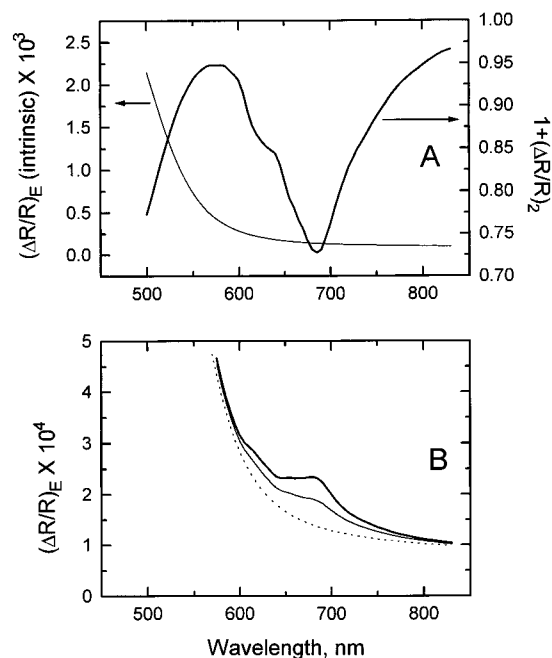


Figure 8. (A) Intrinsic electroreflectance curve of gold based on the model of McIntyre and Aspnes for $\Delta Q_m = +30 \mu\text{C}/\text{cm}^2$ in the region 500–830 nm at $\phi_i = 45^\circ$ (light line, left ordinate). Plot of $1 + (\Delta R/R)_{2s}$ vs λ , where $(\Delta R/R)_{2s}$ is the normalized reflectivity of the Au-(pzc)/PC(1.5 nm)/water at the same angle of incidence (thick line, right ordinate). (B) Electroreflectance curves for the Au(+30 $\mu\text{C}/\text{cm}^2$)/PC-(d_{PC})/water system for $d_{\text{PC}} = 30$ (thin line) and 45 nm (thick line). The dotted line is the intrinsic electroreflectance curve from panel A, for comparison.

very thin layers is twice as small for s-light as for p-polarized light.¹ These are quantitative aspects for which no account can be made with this primitive model.

V. Concluding Remarks

The effects examined in the first part of this work are purely optical in nature, as possible physical and chemical interactions between the constituent phases were completely ignored. The adsorption of species on the surface will, in general, bring about, among other modifications, radical changes in the electronic density at the interface due to the formation of chemical bonds, as well as a net ordering of molecular adsorbates caused by preferred interactions of specific moieties with surface sites. In addition, intermolecular forces, such as those that govern the formation of alkyl-chain-based self-assembled monolayers,¹⁹ can impart a net anisotropy to the adsorbed phase. These electronic and structural effects will alter the optical properties of the two phases in ways that are difficult if not impossible at present to predict strictly on the basis of theory, a factor that complicates even further the interpretation of differential reflectance spectroscopy. Furthermore, the electroreflectance simulations have shown that the changes in the applied potential can give rise to features in the reflectance spectrum that are unrelated to interactions between the field across the interface and the

adsorbate layer. Therefore, an interpretation of experimental data obtained with this technique is by no means straightforward.

It becomes evident from this study that despite the extraordinary sensitivity of optical methods in the UV region, which include spectroscopic ellipsometry,²⁰ the type of information that can be extracted from these data is qualitative at best. Nevertheless, a better understanding of the interplay between the electronic and optical properties of the interface, including the effects of the applied potential, is expected to provide a solid foundation for these methods to reach their full potential.

Acknowledgment. This work was supported in part by ARPA Contract No. N00014-92-J-1848.

References and Notes

- (1) (a) McIntyre, J. D. E. In *Advances in Electrochemistry and Electrochemical Engineering*; Delahay, P., Tobias, C., Eds.; Wiley Interscience: New York, 1973; Vol. 9, p 61. (b) Kolb, D. M. In *Spectroelectrochemistry: Theory and Practice*; Gale, R. J., Ed.; Plenum Press: New York, 1988.
- (2) Kolb, D. M.; Schneider, J. *Electrochim. Acta* **1986**, *31*, 929.
- (3) (a) Kolb, D. M.; Boeck, W.; Ho, K. M.; Liu, S. H. *Phys. Rev. Lett.* **1981**, *47*, 1921. (b) Ho, K. M.; Fu, C. L.; Liu, S. H.; Kolb, D. M.; Piazza, G. *J. Electroanal. Chem.* **1983**, *150*, 235.
- (4) See, for example: Horkans, J.; Cahan, B. D.; Yeager, E. *Surf. Sci.* **1974**, *46*, 1.
- (5) (a) Takamura, T.; Takamura, K.; Yeager, E. *Symp. Faraday Soc.* **1970**, *4*, 91. (b) Mo, Y.; Hwang, E.; Scherson, D. A. *Anal. Chem.* **1995**, *67*, 2415 and references therein.
- (6) (a) Bewick, A.; Thomas, B. *J. Electroanal. Chem.* **1875**, *65*, 911. (b) Ho, F. C.; Conway, B. E.; Angerstein-Kozłowska, H. *Surf. Sci.* **1979**, *81*, 125.
- (7) (a) Ortiz, B.; Park, S. M.; Doddapaneni, N. *J. Electrochem. Soc.* **1996**, *143*, 1800 and references therein. (b) Feng, Z. Q.; Sagara, T.; Niki, K. *Anal. Chem.* **1995**, *67*, 3564 and references therein. (c) Kim, S.; Scherson, D. A. *Anal. Chem.* **1992**, *64*, 3091 and references therein. (d) Kim, S.; Xu, X.; Bae, I. T.; Wang, Z.; Scherson, D. A. *Anal. Chem.* **1990**, *62*, 2647 and references therein.
- (8) Lezna, R. O.; de Tacconi, N. R.; Hahn, F.; Arvia, A. J. *J. Electroanal. Chem.* **1991**, *306*, 259.
- (9) For a rather recent review of this and other *in situ* spectroscopic techniques as applied to the study of electrochemical interfaces, see: Scherson, D.; Yeager, E. In *Investigations of Surfaces and Interfaces-Part B*; Rossiter, B. W., Baetzold, R. C., Eds.; Physical Methods of Chemistry IXB, 2nd ed.; John Wiley & Sons: New York, 1993; Chapter 7.
- (10) (a) Yeh, P. *Surf. Sci.* **1980**, *96*, 41. (b) Yeh, P. *J. Opt. Soc. Am.* **1979**, *69*, 742.
- (11) McIntyre, J. D. E.; Aspnes, D. E. *Surf. Sci.* **1971**, *24*, 417.
- (12) (a) Johnson, L. G.; Dresselhaus, G. *Phys. Rev. B* **1973**, *7*, 2275. (b) Tatar, R. C.; Rabi, S. *Phys. Rev. B* **1982**, *25*, 4126. (c) Randin, J. P.; Yeager, E. *J. Electrochem. Soc.* **1971**, *118*, 711. Randin, J. P.; Yeager, E. *J. Electroanal. Chem.* **1972**, Gerischer, H.; McIntyre, R.; Scherson, D.; Storck, W. *J. Phys. Chem.* **1987**, *91*, 1930.
- (13) See Appendix II in ref 1b.
- (14) Pockrand, L.; Swalen, J. D.; Santo, R.; Brillante, A.; Philpott, M. R. *J. Chem. Phys.* **1978**, *69*, 4001.
- (15) Pribytkova, N. N.; Savostyanova, M. V. *Opt. Spektrosk.* **1966**, 418.
- (16) Dignam, M. J.; Moskovits, M.; Stobe, R. W. *Trans. Faraday Soc.* **1971**, *67*, 3306.
- (17) Schmidt, P. H.; Plieth, W. J. *J. Electroanal. Chem.* **1986**, *201*, 163 and references therein.
- (18) Takamura, T.; Takamura, K.; Watanabe, F. *Surf. Sci.* **1974**, *44*, 93.
- (19) Ulman, A. *Introduction to Ultrathin Organic Films*; Academic Press: San Diego, CA, 1991.
- (20) Gottesfeld, S.; Kim, Y.-T.; Redondo, A. In *Physical Electrochemistry*; Rubinstein, I., Ed.; Marcel Dekker: New York, 1995; Chapter 9.